

Translated from: XIAO Q, HU G Y, XIE J C. Theoretical and experimental research on influencing factors and rules of flow-induced rudder system vibration[J]. Chinese Journal of Ship Research, 2017, 12(1): 84-92, 100.

Theoretical and experimental research on influencing factors and rules of flow-induced rudder system vibration

XIAO Qing, HU Gangyi, XIE Junchao

China Ship Development and Design Center, Wuhan 430064, China

Abstract: Flow-induced rudder system vibration has a great influence on the stealthiness of underwater vehicles. In order to study the vibration characteristics of rudder systems, a mathematical model of a binary linear flutter rudder system is built according to a simplified rudder system structure. Next, the conditions of low speed flutter of the rudder system are determined, and the main influence factors and control rules of the low speed flutter are obtained. In addition, flow-induced vibration tests of the rudder model are made in a gravitation water tunnel, and a study is made of the influences on the rudder system caused by variations in main parameters as support stiffness, torsional stiffness, mass center position and stiffness center position. The results show that the structural design has a great influence on flow-induced rudder system vibration. The flow-induced vibration of the rudder system can be effectively suppressed through the matching design of parameters as the frequency ratio of heave motion and torsion motion, the ratio of structural mass and added mass and the relative positions of the stiffness center, mass center and chord center.

Key words: rudder system; flow-induced vibration; low-speed flutter; water tunnel

CLC number: U664.36

0 Introduction

As a protrusion of underwater vehicle, rudder inevitably vibrates under the induction of flow during the voyage. This vibration will be detrimental to normal operation of the rudder and its transmission system and will have an influence on the stealthiness of underwater vehicle^[1-3].

Based on the relevant research, elastic mechanics theory concerning the rudder wing in the fluid has been basically mature^[4-6]. A lot of calculations and experiments about flow-induced vibration of rudder blade and other airfoil or hydrofoil have been carried out^[7-11]. Based on the above research, this paper studies a kind of rudder blade with small thickness, small camber and small aspect ratio as well as its transmission system. Through theoretical analysis and experiment, the influencing factors and rules of flow-induced rudder system vibration are investigated,

which can provide a guidance for engineering design.

1 Theoretical analysis of flow-induced rudder system vibration

The structure of rudder system of an underwater vehicle is shown in Fig. 1, including rudder blade, rudder axle, sliding bearing, tiller, guide rod, guide device, transmission rod, hydraulic press and so on. Among them, the rudder surface has a hollow variable cross-section; the rudder axle fits with the sleeve, and the axial motion is fixed by the fixed ring. The servo-tiller is used to rotate the rudder surface.

For hydraulic servos, it is assumed that the gap, hydraulic pressure and feedback loops only affect heave and torsional stiffness of the system. The rudder axle and hydraulic servo can be simplified to an

Received: 2016 - 04 - 27

Supported by: National Ministries Foundation

Author(s): XIAO Qing (Corresponding author), male, born in 1979, Ph.D., senior engineer. Research interest: ship equipment.

E-mail: xqzju98@163.com

HU Gangyi, male, born in 1966, Ph.D., professor, doctoral supervisor. Research interest: ship mechanics

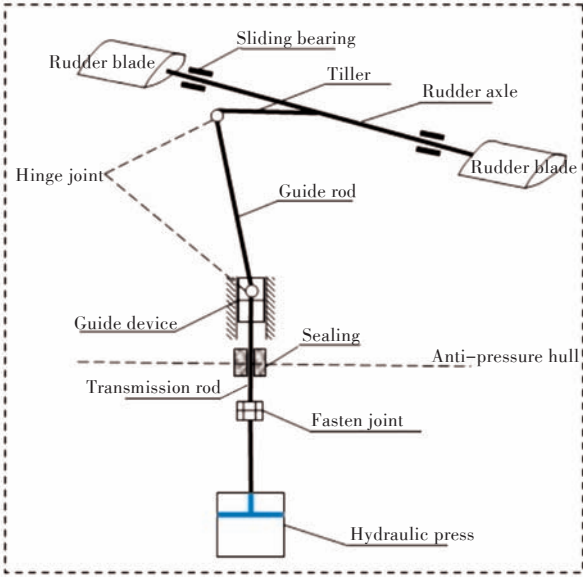


Fig.1 Schematic of the rudder system

equivalent beam $B'B$, and B' and B are connected with the rudder surface. Meanwhile, both ends A' and A installed with bearings are treated as elastic support points to restrain the heave motion of the rudder axle. The connection point O between tiller and rudder axle is treated as fixed end point of elastic torsion, which restrains the torsional motion of the rudder axle, as shown in Fig. 2.

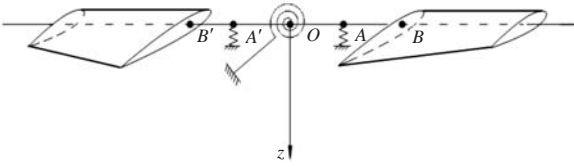


Fig.2 Vibration dynamic model of the rudder system

The rudder axle and rudder blade can be regarded as a rigid body system. A' and A installed with bearings are equivalent to two support springs with heave stiffness of k_h , and the connection point O between tiller and rudder axle is equivalent to a torsion spring, with torsional stiffness of $2k_a$. With the hydrodynamic excitation, rudder blade and rudder stock system has movements of two-degree-of-freedom: one is the heave movement of rudder blade and rudder shock system, with displacement h , and the downward direction is taken as positive; the other is the torsion rotation of rudder blade around rudder axle, with rotation angle α , and the upstream of incident flow is taken as positive.

The heave displacement h and rotation angle α satisfy the following two-degree-of-freedom equations of motion:

$$m \frac{d^2 h}{dt^2} + S_a \frac{d^2 \alpha}{dt^2} + m \omega_h^2 h = -L(t) \quad (1)$$

$$S_a \frac{d^2 h}{dt^2} + I_a \frac{d^2 \alpha}{dt^2} + I_a \omega_a^2 \alpha = M(t) \quad (2)$$

where the system mass is $2m$; the static moment of system mass is $2S_a$; the moment of inertia of the system is $2I_a$; $\omega_a = \sqrt{k_a/I_a}$ refers to the natural frequency of system torsion; $\omega_h = \sqrt{k_h/m}$ refers to the natural frequency of system heave; L refers to the hydrodynamic lift of single rudder blade (the upward direction is taken as positive); M stands for the pitching moment of a single rudder blade (the upstream of incident flow is taken as positive).

When the speed of the underwater vehicle is equal to vibration speed, simple harmonic vibration with the flutter frequency ω happens on the rudder system, namely

$$h = \bar{h}e^{-i\omega t}, \alpha = \bar{\alpha}e^{-i\omega t} \quad (3)$$

The corresponding lift and pitching moment can be written as

$$L = \bar{L}e^{-i\omega t}, M = \bar{M}e^{-i\omega t} \quad (4)$$

Substituting Eq. (3) and Eq. (4) into Eq. (1) and Eq. (2), there are:

$$-m\omega^2 \bar{h} - S_a \omega^2 \bar{\alpha} + m\omega_h^2 \bar{h} = -\bar{L} \quad (5)$$

$$-S_a \omega^2 \bar{h} - I_a \omega^2 \bar{\alpha} + I_a \omega_a^2 \bar{\alpha} = \bar{M} \quad (6)$$

For hydrofoils with small thicknesses, small camber and unlimited span, the unsteady hydrodynamic lift and pitching moment can be determined by Teodorsen theory when subjected to simple harmonic heave and torsion motion in incompressible flow at a given angle of attack. However, the rudder system in this study belongs to hydrofoil with small aspect ratio, small thickness and small camber. When calculating the unsteady hydrodynamic lift and pitching moment, it is necessary to consider the three-dimensional effect of the rudder blade, namely the Teodorsen theory needs to be corrected.

Supposing the density of water being ρ_w , the half chord length of the rudder blade being b , and the span being l , and \bar{a} is the percentage of distance from the center of the rudder blade section to the stiffness center (the position of the spin axis) in the half of chord length. If the stiffness center is behind the center of rudder section (Fig. 3), \bar{a} is positive. Thus, hydrodynamic lift and pitching moment of rudder blade with limited span can be expressed as

$$\begin{aligned} -\bar{L} &= P(\bar{h}/b) + Q\bar{\alpha} \\ \bar{M} &= R(\bar{h}/b) + T\bar{\alpha} \end{aligned} \quad (7)$$

where

$$P = \pi \rho_w b^3 l \omega^2 L_h \quad (8)$$

$$Q = \pi \rho_w b^3 l \omega^2 [L_a - (0.5 + \bar{a})L_h] \quad (9)$$

$$R = \pi \rho_w b^4 l \omega^2 [M_h - (0.5 + \bar{a})L_h] \quad (10)$$

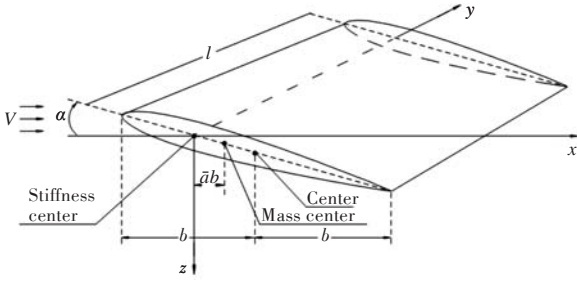


Fig.3 Hydrodynamic calculation model of the limited span rudder blade

$$T = \pi \rho_w b^4 l \omega^2 [M_a - (0.5 + \bar{a})(L_h + M_h) + (0.5 + \bar{a})^2 L_h] \quad (11)$$

The parameters in Eq. (8)–Eq. (11) are as follows:

$$L_h = \varepsilon - \frac{2\delta C(k)}{k} \mathbf{i}$$

$$L_a = \frac{\varepsilon}{2} - \frac{\varepsilon + 2\delta C(k)}{k} \mathbf{i} - \frac{2\delta C(k)}{k^2} \quad (12)$$

$$M_a = \left(\frac{3}{8} - \frac{\mathbf{i}}{k} \right) \varepsilon \quad (13)$$

$$M_h = \frac{\varepsilon}{2} \quad (14)$$

In Eq. (12): ε refers to the correction parameter of added mass, $\varepsilon = \frac{l}{\sqrt{b^2 + l^2}}$; $k = \omega b / v$ refers to the reduced frequency, v refers to the speed of underwater vehicle; $C(k)$ refers to Teodorsen function, which can be expressed as

$$C(k) = \frac{H_1^{(2)}(k)}{H_1^{(2)}(k) + \mathbf{i}H_0^{(2)}(k)} \quad (15)$$

$H_v^{(2)}$ stands for the second class v -order Hankel function.

In Eq. (12), δ refers to correction parameter of circulation.

$$\delta = \frac{\pi}{4} \left(1 + 2 \frac{\tau}{AR} \right) \quad (16)$$

AR refers to aspect ratio; τ refers to shape parameter (related to AR), as shown in Fig. 4.

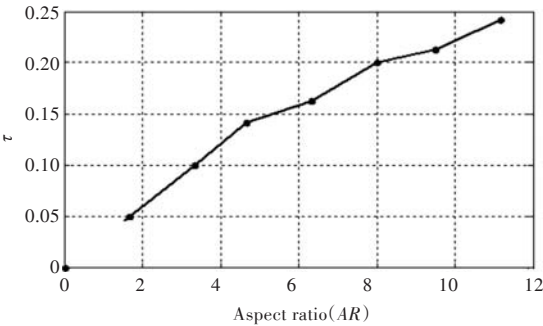


Fig.4 Relationship between AR and τ

Eq. (5) and Eq. (6) can be expressed as matrix equation:

$$-\omega^2 \mathbf{N} \begin{bmatrix} \bar{h}/b \\ \bar{\alpha} \end{bmatrix} + \mathbf{K} \begin{bmatrix} \bar{h}/b \\ \bar{\alpha} \end{bmatrix} = \omega^2 \mathbf{A}(k) \begin{bmatrix} \bar{h}/b \\ \bar{\alpha} \end{bmatrix} \quad (17)$$

where

$$\begin{aligned} \mathbf{N} &= \begin{bmatrix} mb & S_a \\ S_a b & I_a \end{bmatrix} \\ \mathbf{K} &= \begin{bmatrix} m\omega_h^2 b & 0 \\ 0 & I_a \omega_a^2 \end{bmatrix} \\ \mathbf{A}(k) &= \begin{bmatrix} P & Q \\ R & T \end{bmatrix} \end{aligned} \quad (18)$$

The $v-g$ method is one of the most commonly used methods in flutter analysis. In this method, it is firstly assumed that the system damping is zero and then artificial damping is introduced in the motion equation of system. Then, Eq. (7) can be transformed into

$$-\omega^2 \mathbf{N} \begin{bmatrix} \bar{h}/b \\ \bar{\alpha} \end{bmatrix} + (1 + \mathbf{i}g) \mathbf{K} \begin{bmatrix} \bar{h}/b \\ \bar{\alpha} \end{bmatrix} = \omega^2 \mathbf{A}(k) \begin{bmatrix} \bar{h}/b \\ \bar{\alpha} \end{bmatrix} \quad (19)$$

Arranging the above equation into a generalized eigenvalue problem, which is shown as follows:

$$(\mathbf{A}(k) + \mathbf{N}) \begin{bmatrix} \bar{h}/b \\ \bar{\alpha} \end{bmatrix} = \frac{(1 + \mathbf{i}g)}{\omega^2} \mathbf{K} \begin{bmatrix} \bar{h}/b \\ \bar{\alpha} \end{bmatrix} \quad (20)$$

Its eigenvalue is

$$\lambda = \frac{(1 + \mathbf{i}g)\omega_a}{\omega^2} = \lambda_{\text{Re}} + \mathbf{i}\lambda_{\text{Im}} \quad (21)$$

Thus

$$\omega = \frac{\omega_a}{\sqrt{\lambda_{\text{Re}}}}, g = \frac{\lambda_{\text{Im}}}{\lambda_{\text{Re}}} \quad (22)$$

Since the reduced frequency $k = \omega b / v$, there is

$$v = \frac{b\omega_a}{k\sqrt{\lambda_{\text{Re}}}} \quad (23)$$

The specific procedures of flutter analysis by $v-g$ method are as follows:

1) By solving the generalized eigenvalue problem (Eq. (20)), the change functions of g , v and ω with k are obtained and then the $v-g$ and $v-\omega$ functions are drawn.

2) When $g = 0$, the system is in a critical state and the flutter just occurs. The v at this time is the flutter velocity v_F and ω is the flutter frequency;

3) When $g < 0$, the system is stable and no flutter occurs;

4) When $g > 0$, the system is unstable and flutter has occurred already.

The flutter of underwater vehicle usually occurs when the mass is relatively small. At this time, when flow velocity is less than the flutter velocity, the system is already divergent, so such flutter is usually dangerous for low-speed underwater vehicle. The rudder of underwater vehicle is a kind of low mass ratio system and its rudder flutter belongs to low-speed flutter problem.

2 Characteristic analysis of rudder blade flutter of underwater vehicle

2.1 Analysis parameter

According to the above calculation theory, the following parameters can be obtained by modeling the rudder blade of underwater vehicle and calculating the wet mode of the whole simplified rudder system.

- 1) Span: $l = 3.19$ m;
- 2) Rudder blade mass + water mass + interior rudder axle mass: $m_{\text{total}} = 3\,202$ kg;
- 3) Half chord length at 3/4 of wing span: $b = 0.9$ m;
- 4) Half chord length of wing panel at mass center position: $b_{\text{cg}} = 1.043\,5$ m;
- 5) Mass per unit span: $m = m_{\text{total}}/l = 1\,003$ kg/m;
- 6) Dimensionless magnitude of the distance from mass center to center: $\varepsilon_{\text{cg}} = -0.157\,7$;
- 7) Dimensionless magnitude of the distance from stiffness center to center: $a = -0.48$;
- 8) Dimensionless magnitude of the distance from stiffness center to mass center: $x_a = 0.322\,3$;
- 9) Mass static moment of per unit rudder blade span with respect to stiffness center: $S_a = 291.16$ kg ;
- 10) Mass moment of inertia of per unit rudder blade span with respect to stiffness center can be approximately equal to: $I_a = 371.3$ kg · m ;
- 11) Dimensionless turning radius of rudder blade with respect to stiffness center: $r_a = 0.583$;
- 12) Dimensionless magnitude of frequency ratio: $R_\omega = \omega_n/\omega_a$;
- 13) Dimensionless mass: $\mu = m/(\pi\rho_w b^2) = 0.395$.

There are five dimensionless parameters for calculation of linear flutter, namely a , μ , r_a , x_a , R_ω . Their initial values are: $a = -0.48$, $\mu = 0.395$, $r_a = 0.583$, $x_a = 0.322\,3$, $R_\omega = 0.549\,9$.

2.2 Characteristic analysis

By analyzing the flutter characteristics of the rudder system, it can be seen that heave stiffness, torsional stiffness, relative position of rudder blade pressure center, stiffness center and mass center, as well as the ratio of concentrated mass to added mass of the rudder have significant effects on the low-speed flutter of rudder. In order to study the influence of these factors on the low-speed flutter of the rudder, the values of a , μ , r_a , x_a and R_ω are changed according to calculation model of low-speed flutter to calculate the flutter speed.

It can be seen from Fig. 5 and Fig. 6 that when x_a is between -0.2 and 0 , no flutter occurs, indicating that the mass center coincides with the stiffness center or the mass center is in front of the stiffness center. Moreover, flutter does not occur when the dimensionless mass ratio changes from 0 to 50 .

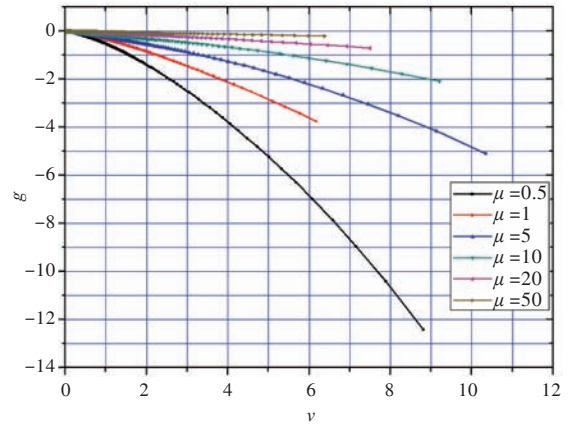


Fig.5 Relationship between velocity and artificial damping ($x_a = -0.2$)

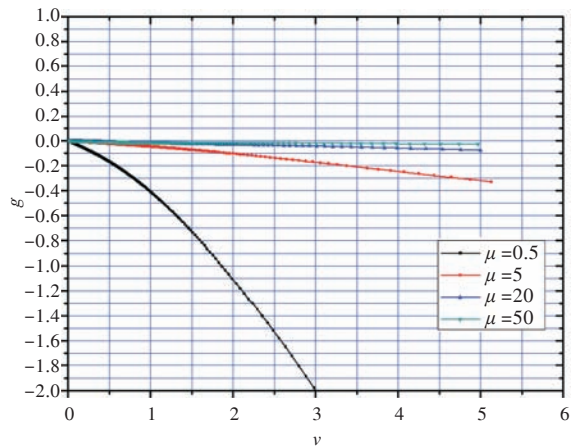


Fig.6 Relationship between velocity and artificial damping ($x_a = 0$)

It can be seen from Fig. 7 that when x_a is reduced, the critical flutter speed can be effectively improved, and when x_a is reduced to a certain extent, flutter will be difficult to occur. In addition, each curve has a minimum value μ_m . When $\mu \leq \mu_m$, with $\mu \rightarrow 0$, flutter speed will rise with a steep slope and flutter is difficult to happen. When $\mu > \mu_m$, with the increase of μ , flutter speed increases slowly and flutter is easy to happen. Therefore, under normal circumstances, for a given structure with unchanged m and ω_a , the rudder mass in high-density medium is relatively small and there is little risk of flutter.

It can be noted from Fig. 8 that the flutter velocity is close to the minimum when the frequency ratio R_ω approaches to 1. If ω_n is increased and R_ω is con-

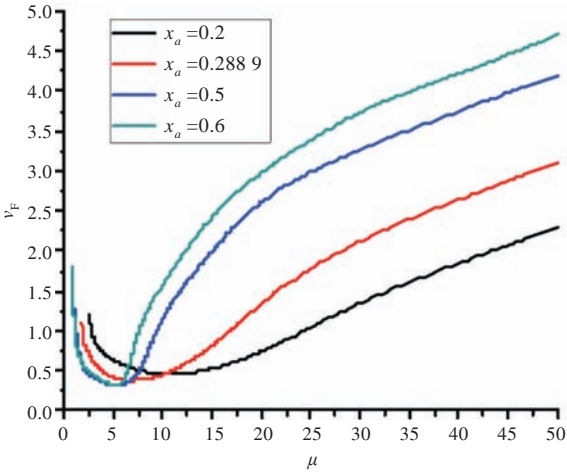
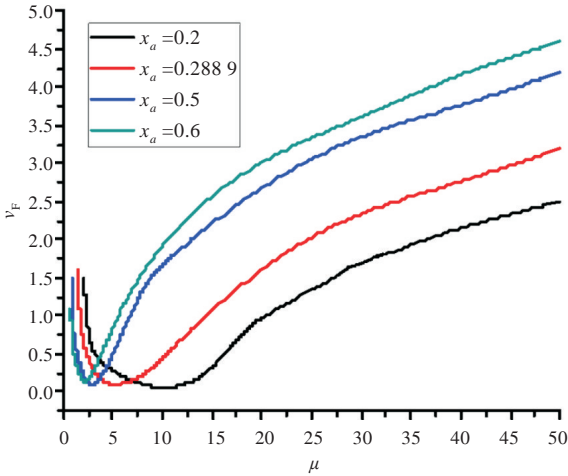
(a) $a = -0.48$ (b) $a = -0.3$

Fig.7 Influencing rules of mass ratio to flutter velocity
($r_a = 1.06, R_\omega = 0.9722$)

stant, v_F will increase proportionally with ω_a . When $R_\omega < 1$, if ω_a is increased separately, the value of v_F will be greatly increased due to decrease of R_ω . If ω_h is increased, v_F is reduced accordingly when $R_\omega < 1$. It can be seen that the main flutter mode is torsional mode, which means that the torsional branch becomes unstable firstly for the current parameter combination. So, flutter velocity can be increased greatly by increasing the torsional stiffness. In addition, v_F can be increased by advancing the dimensionless x_a of mass center with respect to stiffness center. In general, mass center can be moved forward by increasing the counterweight at the front of the hydrofoil.

3 Experimental research on flow-induced rudder system vibration

In order to further study influencing factors of flow-induced rudder system vibration, experimental

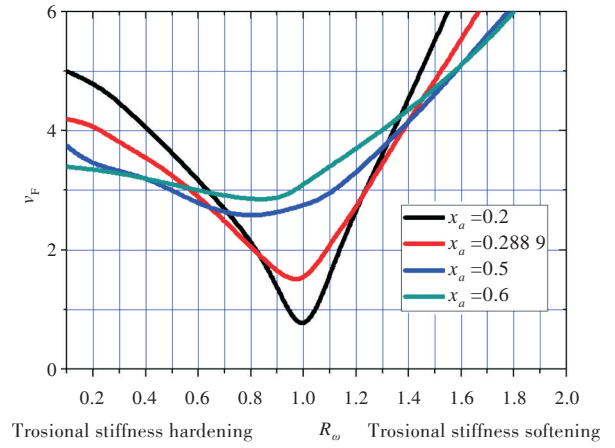
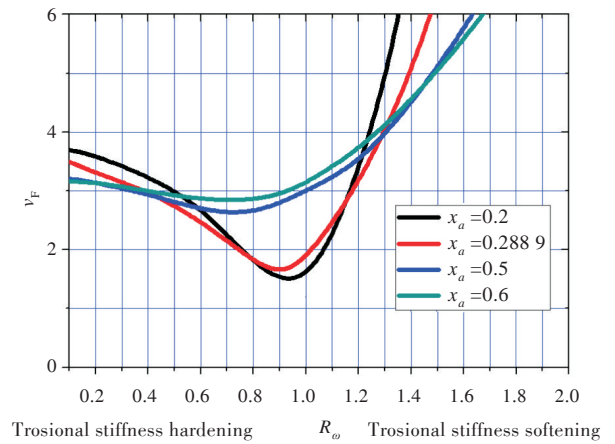
(a) $a = -0.48$ (b) $a = -0.3$

Fig.8 Influencing rules of frequency ratio to flutter velocity
($r_a = 1.06, \mu = 20$)

research on flow-induced rudder system vibration are carried out on the basis of previous sections.

3.1 Experiment model

The experiment model consists of three parts: rudder blade, rudder axle and trestle.

Considering two rudder blade models, one is with the constant cross-section and the other is with the variable cross-section. The rudder blade model with constant cross-section is the NACA0017 airfoil made of stainless steel. The skin thickness is 0.5 mm and the chord is 1 mm. 1/4, 1/2 and 3/4 of the span is supported by 1 mm rib, respectively.

The molded lines of rudder blade are shown in Fig. 9 and specific parameters of the rudder blade are listed in Table 1. When the stiffness center is behind the chord midpoint, $\bar{a} > 0$; when the mass center is behind the stiffness center, $x_a > 0$.

The section of rudder blade with variable cross-section still adopts NACA0017 airfoil, which is made of plastic and has a hollow interior. The

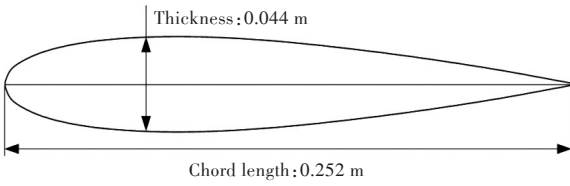


Fig.9 Molded lines of the constant cross-section rudder

Table 1 Parameters of the constant cross-section rudder

| Parameter | Value |
|---|-------|
| Mass m/kg | 2.9 |
| Span l/m | 0.39 |
| Half of chord length b/m | 0.126 |
| The ratio of distance from chord midpoint to the stiffness center to half of the chord length \bar{a} | -0.48 |
| The distance from mass center to stiffness center x_a/m | 0.042 |

weight is used to adjust the mass and mass center, as shown in Fig. 10. The specific parameters of the rudder are shown in Table 2.

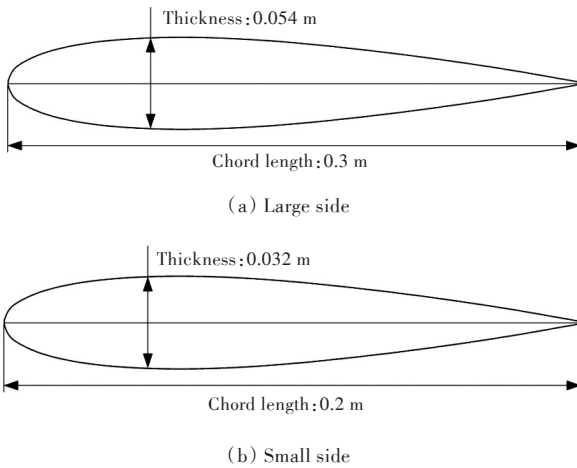


Fig.10 Molded lines of the variable cross-section rudder

Table 2 Parameters of the variable cross-section rudder

| | |
|----------------|------------|
| m/kg | 2.84 |
| l/m | 0.39 |
| b/m | 0.129 |
| \bar{a} | -0.48 |
| x_a/m | 0.035~0.05 |

In the test model, support stiffness of rudder bearing can be adjusted by adjustable support structure (Fig. 11), and four sets of springs are arranged at the rudder stock to adjust the torsional stiffness and rudder angle. In order to simulate different positions of mass center and stiffness center, a number of rudder structure models are fabricated. The internal hollow structure is adopted and the parameters such as structural mass and mass center position of the rudder are adjusted by the weight.

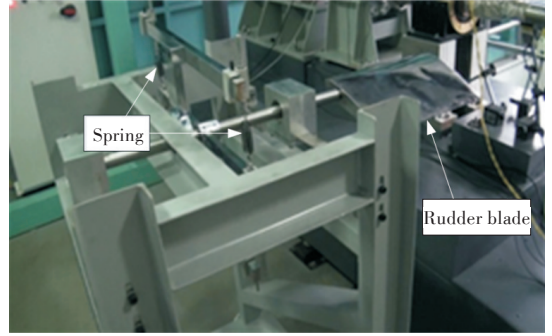


Fig.11 Experimental model

Supporting spring fixed between the trestle and the rudder axle structure is used to simulate support stiffness. The rudder axle structure contains bearings so as not to restrain the torsion of rudder axle. When the axle is subjected to flow-induced heave motion, the spring will produce reaction force to simulate the support stiffness. The magnitude of support stiffness is mainly achieved by changing the stiffness of support spring. Torsional stiffness can be simulated by a set of springs perpendicular to rudder torsion bar and can be changed by adjusting the distance from the spring to the axle.

3.2 Experimental conditions

The gravitation water tunnel is used to study characteristics of flow-induced vibration of rudder-rod model system and to test the flow-induced vibration response of test model under different combined conditions, as well as to know the flow-induced vibration characteristics of the rudder system. The working section of water tunnel is 6.0 m long. The cross-section is 0.7 m \times 0.7 m. The maximum water velocity is 5 m/s. The unevenness of flow velocity is less than 1% and the turbulence intensity is less than 0.5%, as shown in Fig. 12.



Fig.12 Gravitation water tunnel

3.3 Experimental methods

Test trestle (including supporting steel and torsion springs, etc.) is placed outside the water tunnel, and the rudder blade is placed inside water tunnel (the

rudder blade is 5 cm from the side of water tunnel). According to experiment requirements, rudder angle of attack, support stiffness and torsional stiffness are adjusted, and then the pump of water tunnel is opened. In addition, flow velocity within experimental section is recorded by pitot tube, which increases gradually in accordance with certain interval. Meanwhile, vibration data of rudder rod system under different flow velocities are recorded. The vibration of test system is measured by using laser vibrometer and acceleration sensor.

3.4 Experimental results

3.4.1 Influence rules of support stiffness on rudder model vibration

Adjusting the support stiffness of test trestle to be $k_h = 9.0 \times 10^4, 3.0 \times 10^5, 1.5 \times 10^6$ N/m, which is selected according to actual situations. The flow-induced vibration test is carried out at different speeds. The other parameters are: $\alpha = 5^\circ, k_a = 282$ (N·m)/rad, $\bar{a} = -0.48, x_a = 0.042$ m. The influence rules of support stiffness on the vibration amplitude and frequency of rudder model are measured.

From the results shown in Fig. 13, it can be seen that the heave and torsional vibration frequency vary with flow velocity under different support stiffness. In addition, heave and torsional vibration frequencies vary close to their natural frequencies, namely both of them are low-frequency vibrations in the vicinity of their respective natural frequencies. Moreover, the greater the support stiffness is, the greater the heave motion frequency of rudder system is, but the smaller the torsional motion frequency is.

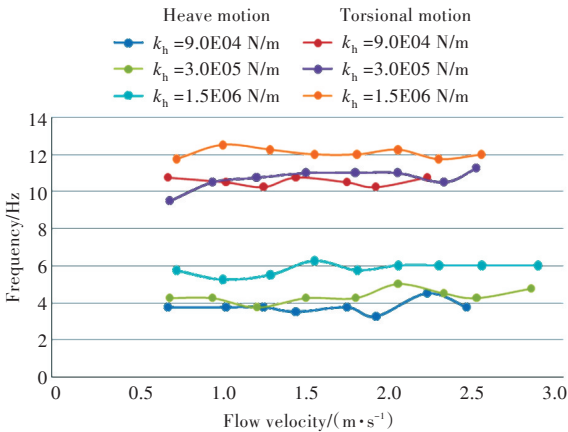


Fig.13 The varying characteristics of rudder system motion frequency under different support stiffness

Fast Fourier transform of the signals collected by acceleration sensors on rudder surface with different support stiffness at $v = 2.03$ m/s is performed, and

the varying curves of heave motion acceleration in frequency domain are shown in Fig. 14. At the same time, fast Fourier transform of the signals collected by acceleration sensors on torsion bar under different support stiffness at the same flow velocity is also conducted, and the varying curves of torsion motion acceleration in frequency domain are shown in Fig. 15.

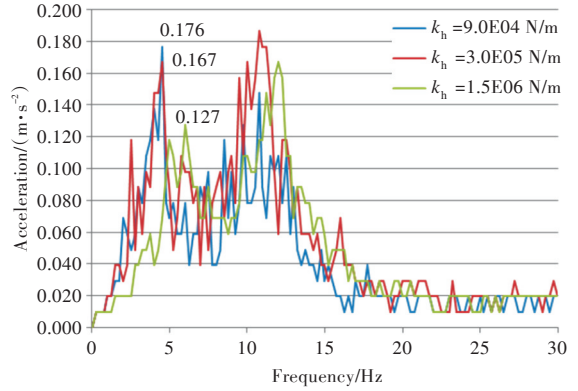


Fig.14 The varying characteristics of heave motion acceleration under different support stiffness($v = 2.03$ m/s)

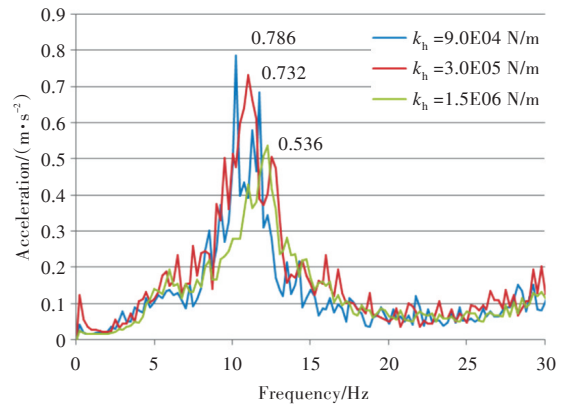


Fig.15 The varying characteristics of torsion motion acceleration under different support stiffness($v = 2.03$ m/s)

Through analysis of Fig. 14 and Fig. 15, under the same flow velocity, the larger the support stiffness is, the smaller the amplitudes of heave motion and torsional motion of rudder blade are, and the effect on the first-order heave motion is largest. Therefore, support stiffness has the greatest influence on heave and torsion motion of the rudder blade, and the increase of support stiffness in a certain range is helpful to control flow-induced vibrations of the rudder.

3.4.2 Influence rules of torsional stiffness on rudder model vibration

The torsional stiffness $k_a = 282, 704, 1\ 348$ N·m/rad is selected by adjusting torsional stiffness of test trestle according to the actual situation. The flow-induced vibration test is carried out at different speeds. The other parameters are: $\alpha = 5^\circ, k_h = 1.5 \times$

10^6 N/m, $\bar{a} = -0.48$, $x_a = 0.042$ m, and the influence rules of torsional stiffness change on amplitude and frequency of rudder model vibration are measured.

Fig. 16 shows the varying characteristics of heave and torsional vibration frequency of rudder system with flow velocity under different torsional stiffness conditions. It can be seen from the figure that the heave and torsional vibration frequencies vary in the vicinity of their natural frequencies. With the increase of torsional stiffness, the torsional motion frequency gradually increases, while the heave motion frequency does not have obvious change.

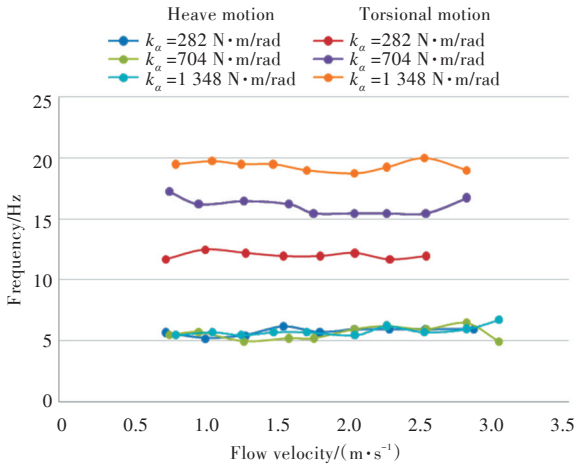


Fig.16 The varying characteristics of rudder system motion frequency under different torsional stiffness

Fast Fourier transform of the signals collected by acceleration sensors on rudder surface with different torsional stiffness at $v = 2.03$ m/s is carried out. The varying curves of heave motion acceleration in frequency domain are shown in Fig. 17. Fast Fourier transform of the signals collected by acceleration sensors on torsion bar under different torsional stiffness at the same flow velocity is conducted, and the varying curves of torsion motion acceleration in frequency domain are shown in Fig. 18.

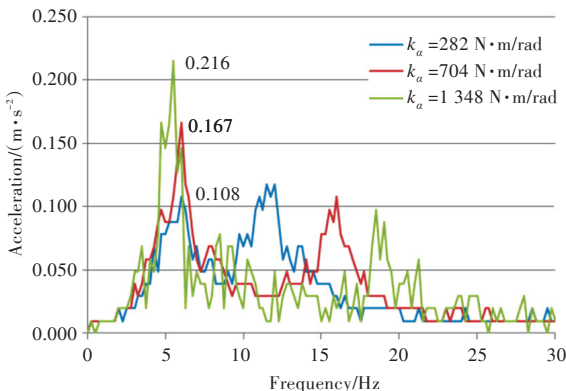


Fig.17 The varying characteristics of heave motion acceleration under different torsional stiffness ($v = 2.03$ m/s)

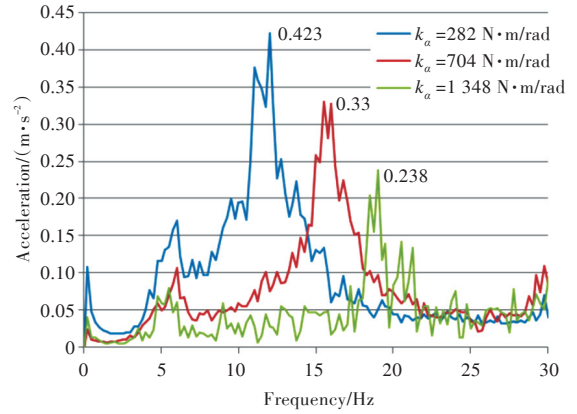


Fig.18 The varying characteristics of torsion motion acceleration under different torsional stiffness ($v = 2.03$ m/s)

According to the analysis of Fig. 17 and Fig. 18, it can be seen that the increase of torsional stiffness has a significant suppression effect on the maximum amplitude of torsion motion of the rudder blade, but the amplitude of first-order heave motion will increase.

3.4.3 Influence rules of stiffness center position on rudder model vibration

By adjusting the distance from the stiffness center to chord midpoint, the flow-induced vibration experiment of rudder model is carried out at different speeds, respectively. According to the actual situation, stiffness center positions $\bar{a} = -0.24, -0.48, -0.81$ are selected and the other parameters are: $\alpha = 5^\circ$, $k_h = 1.5 \times 10^6$ N/m, $k_a = 282$ (N·m)/rad, $x_a = 0.042$ m. The influence rules of distance change from stiffness center to chord midpoint on vibration amplitude and frequency of rudder model are measured.

The varying characteristics of heave and torsional vibration frequencies in rudder system with flow velocity at different stiffness center positions are shown in Fig. 19, when $\alpha = 5^\circ$, $k_h = 1.5 \times 10^6$ N/m, $k_a = 282$ (N·m)/rad, $x_a = 0.042$ m. The figure shows that the heave and torsional vibration frequencies vary in the vicinity of their respective natural frequencies, namely these two kinds of flow-induced vibrations belong to low-frequency vibration near their respective natural frequencies. On the whole, when stiffness center is closest to guide margin ($\bar{a} = -0.81$), the torsional motion frequency is the largest while the heave motion frequency is the smallest.

Fast Fourier transform of the signals collected by acceleration sensors on the rudder surface under different stiffness center positions at specific flow velocity ($v = 2.03$ m/s) is performed, and the varying curves of heave motion acceleration in frequency domain are shown in Fig. 20. Fast Fourier transform of

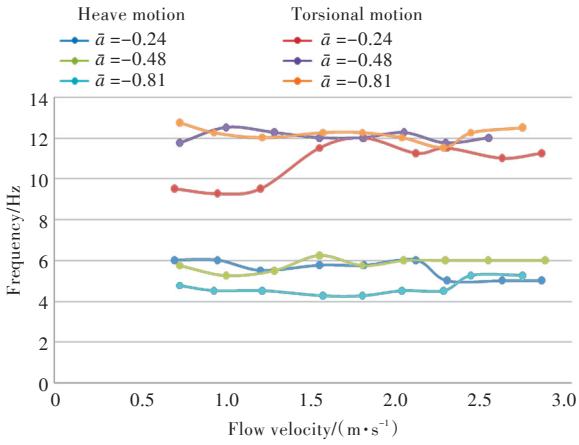


Fig.19 The varying characteristics of rudder system motion frequency under different stiffness center positions

the signals collected by acceleration sensors on torsional bar under different stiffness center positions at the same flow velocity is conducted, and the varying curves of torsional motion acceleration in frequency domain are shown in Fig. 21.

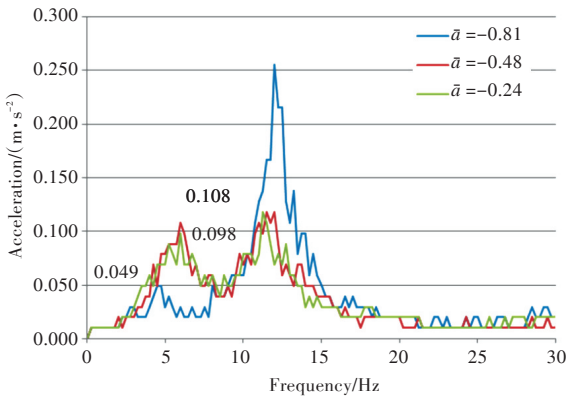


Fig.20 The varying characteristics of heave motion acceleration under different stiffness center positions($v = 2.03$ m/s)

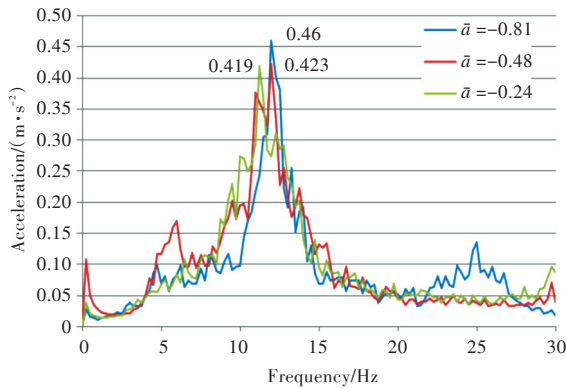


Fig.21 The varying characteristics of torsion motion acceleration under different stiffness center positions($v = 2.03$ m/s)

According to the analysis of Fig. 20 and Fig. 21, it can be seen that the reduction of the distance from stiffness center position to guide margin has obvious suppression effect on the maximum amplitude of heave motion of the rudder blade and unobvious ef-

fect on the maximum amplitude of torsional motion, but increases the torsional vibration frequency.

3.4.4 Influence rules of mass center position on rudder model vibration

By adjusting the mass center position, the mass center positions $x_a = 0.03, 0.042, 0.05$ m are respectively selected for flow-induced vibration experiments of rudder model under different speeds according to the actual situation. The other parameters are: $\alpha = 5^\circ$, $k_h = 1.5 \times 10^6$ N/m, $k_a = 282$ (N · m)/rad, $\bar{a} = -0.48$. The influence rules of varying mass center position on the amplitude and frequency of rudder model vibration are measured.

Fig. 22 shows the varying characteristics of heave and torsional frequencies of rudder system with flow velocity under different mass center positions, when $\alpha = 5^\circ$, $k_h = 1.5 \times 10^6$ N/m, $k_a = 282$ (N · m)/rad, $\bar{a} = -0.48$. The figure shows the frequencies of heave and torsional vibration change in the vicinity of their respective natural frequencies, indicating that both types of flow-induced vibration belong to low-frequency vibration in the vicinity of their respective natural frequencies.

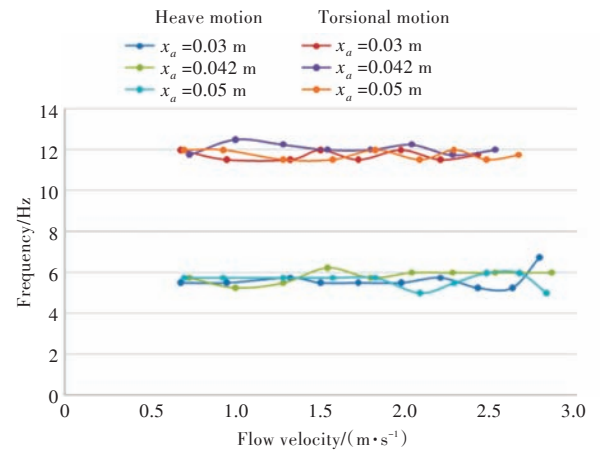


Fig.22 The varying characteristics of rudder system motion frequency under different mass center positions

Fast Fourier transform of the signals collected by acceleration sensors on rudder surface under different mass center positions at specific speed $v = 2.03$ m/s is carried out, and the varying curves of heave motion acceleration in frequency domain are shown in Fig. 23. Moreover, fast Fourier transform of the signals collected by acceleration sensors on torsion bar under different mass center positions at the same flow velocity is conducted, and the varying curves of torsional motion acceleration in frequency domain are shown in Fig. 24.

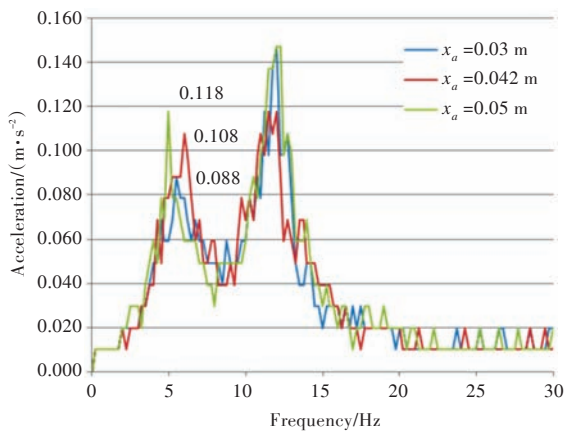


Fig.23 The varying characteristics of heave motion acceleration under different mass center positions($v=2.03$ m/s)

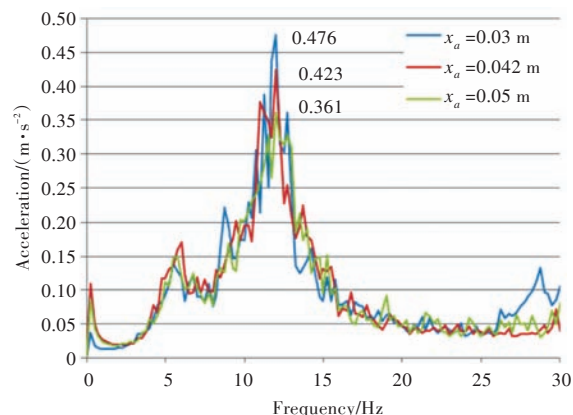


Fig.24 The varying characteristics of torsion motion acceleration under different mass center positions($v=2.03$ m/s)

According to the analysis of Fig. 23 and Fig. 24, it can be seen that under the same flow velocity, the larger the distance from mass center to stiffness center is (the mass center is behind the stiffness center), the larger the amplitude of rudder heave motion is, while the amplitude of torsional motion is relatively reduced. Therefore, the smaller the distance from mass center to stiffness center is, the more favorable the control of heave motion of rudder blade is.

4 Conclusions

Through establishing the experiment models of flow-induced rudder system vibration with adjustable parameters, a series of experiments are carried out. It can be found that experimental results are basically consistent with theoretical trends. The main conclusions are as follows:

1) Increasing the support stiffness can significantly reduce acceleration amplitude of heave vibration in rudder system, so support stiffness can be increased as much as possible in the design.

2) Although increasing the torsional stiffness can reduce the acceleration amplitude of torsional vibra-

tion, it also increases the acceleration amplitude of heave vibration. Therefore, reasonable selection of torsional stiffness is critical in the design, and the bigger does not mean the better.

3) The effect of stiffness center position on acceleration amplitude of torsional vibration in rudder system is not significant, but if stiffness center position moves forward properly, acceleration amplitude of heave vibration in rudder system can be significantly reduced. Therefore, stiffness center position can be properly moved forward under the premises of ensuring system stability and related hydrodynamic and structural performance.

4) The effect of mass center position on acceleration amplitude of torsional vibration in rudder system is not significant. If the mass center position is properly moved forward at low-speed condition, acceleration amplitude of heave vibration can be reduced.

In this study, calculation model of flow-induced rudder system vibration is established, and theoretical calculation is carried out to analyze the influencing factors and the functional rules of low-speed flutter of the rudder. In addition, the flow-induced vibration test is conducted to study the influencing factors and rules of flow-induced rudder system vibration, which can provide a reference for the design of flow-induced rudder system vibration in engineering development.

At the same time, it can be seen that due to the limited test conditions, the equivalent reduced scale of the model is large, and nonlinear factors such as gap and friction cannot be treated completely and equivalently in the test system, having certain influence on the test results. The experimental results and theoretical calculation cannot be compared and verified quantitatively. Therefore, it is necessary to study the influence of nonlinear factors on the quantification of flow-induced vibration.

References

- [1] WANG C X, WU C J, CHEN L J, et al. A comprehensive review on the mechanism of flow-induced noise and related prediction methods [J]. Chinese Journal of Ship Research, 2016, 11(1): 57-71 (in Chinese).
- [2] YU M S, WU Y S, PANG Y Z. A review of progress for hydrodynamic noise of ships [J]. Journal of Ship Mechanics, 2007, 11(1): 152-158 (in Chinese).
- [3] Blevins R D. Flow-induced vibration [M]. Translated by Wu S S, Beijing: China Machine Press, 1983 (in Chinese).
- [4] Forschung H W. 气动弹性力学原理 [M]. Translated

